JOURNAL OF GEOPHYSICAL RESEARCH, VOL. 115, C03024, doi:10.1029/2009JC005267, 2010

Seasonal forcing of summer dissolved inorganic carbon and chlorophyll *a* on the western shelf of the Antarctic Peninsula

Martin Montes-Hugo,[1] Colm Sweeney,[2] Scott C. Doney,[3] Hugh Ducklow,[4] Robert Frouin,[5] Douglas G. Martinson,[6] Sharon Stammerjohn,[7] and Oscar Schofield[1]

Received 7 January 2009; revised 19 October 2009; accepted 3 November 2009; published 30 March 2010.

[1] The Southern Ocean is a climatically sensitive region that plays an important role in the regional and global modulation of atmospheric CO_2. Based on satellite-derived sea ice data, wind and cloudiness estimates from numerical models (National Centers for Environmental Prediction-National Center for Atmospheric Research reanalysis), and in situ measurements of surface (0–20 m depth) chlorophyll *a* (Chl_{Surf}) and dissolved inorganic carbon (DIC_{Surf}) concentration, we show sea ice concentration from June to November and spring wind patterns between 1979 and 2006 had a significant influence on midsummer (January) primary productivity and carbonate chemistry for the Western Shelf of the Antarctic Peninsula (WAP, 64°–68°S, 63.4°–73.3°W). In general, strong (>3.5 m s^{-1}) and persistent (>2 months) northerly winds during the previous spring were associated with relatively high (monthly mean > 2 mg m^{-3}) Chl_{Surf} and low (monthly mean < 2 mmol kg^{-1}) salinity-corrected DIC (DIC_{Surf}*) during midsummer. The greater Chl_{Surf} accumulation and DIC_{Surf}* depletion was attributed to an earlier growing season characterized by decreased spring sea ice cover or nearshore accumulation of phytoplankton in association with sea ice. The impact of these wind-driven mechanisms on Chl_{Surf} and DIC_{Surf}* depended on the extent of sea ice area (SIA) during winter. Winter SIA affected phytoplankton blooms by changing the upper mixed layer depth (UMLD) during the subsequent spring and summer (December–January–February). Midsummer DIC_{Surf}* was not related to DIC_{Surf}* concentration during the previous summer, suggesting an annual replenishment of surface DIC during fall/winter and a relatively stable pool of deep (>200 m depth) "winter-like" DIC on the WAP.

Citation: Montes-Hugo, M., C. Sweeney, S. C. Doney, H. Ducklow, R. Frouin, D. G. Martinson, S. Stammerjohn, and O. Schofield (2010), Seasonal forcing of summer dissolved inorganic carbon and chlorophyll *a* on the western shelf of the Antarctic Peninsula, *J. Geophys. Res.*, *115*, C03024, doi:10.1029/2009JC005267.

1. Introduction

[2] The Western Shelf of the Antarctic Peninsula (WAP), in the Bellingshausen Sea, is a region that is very sensitive to climate change and has experienced in the last few decades some of the greatest winter atmospheric warming (>0.5°C per decade) on Earth [*Vaughan et al.*, 2003]. These air temperature trends have been accompanied by an abbreviated sea ice season [*Stammerjohn and Smith*, 1997] and the progressive replacement of polar climate characterized by warmer subpolar conditions [*Smith et al.*, 2003]. These climate shifts have been associated with large modifications in phytoplankton communities [*Ducklow et al.*, 2006; *Montes-Hugo et al.*, 2009], thus potential variations in seawater carbonate system are expected since phytoplankton is a major biological factor modulating the amount of inorganic carbon in the euphotic zone of the WAP region [*Carrillo and Karl*, 1999; *Carrillo et al.*, 2004]. Phytoplankton photosynthesis decreases the total dissolved inorganic carbon (DIC), by depleting aqueous CO_2, and increases the net community production (NCP) (i.e., primary production minus community respiration). In the surface mixed layer of the WAP region, annual NCP corrected by air-sea CO_2 exchange is relatively high (>6 mol C m^{-2} y^{-1}) with respect to other oceanic regions [*Lee*, 2001], suggesting

[1]Coastal Ocean Observation Lab, Institute of Marine and Coastal Sciences, School of Environmental and Biological Sciences, Rutgers-State University of New Jersey, New Brunswick, New Jersey, USA.
[2]Global Monitoring Division, Earth Systems Research Laboratory, National Oceanic and Atmospheric Administration, Boulder, Colorado, USA.
[3]Department of Marine Chemistry and Geochemistry, Woods Hole Oceanographic Institution, Woods Hole, Massachusetts, USA.
[4]Ecosystems Center, Marine Biological Laboratory, Woods Hole, Massachusetts, USA.
[5]Scripps Institution of Oceanography, University of California, San Diego, La Jolla, California, USA.
[6]Lamont-Doherty Earth Observatory, Department of Earth and Environmental Sciences, Columbia University, Palisades, New York, USA.
[7]Ocean Sciences, University of California, Santa Cruz, California, USA.

0148-0227/10/2009JC005267

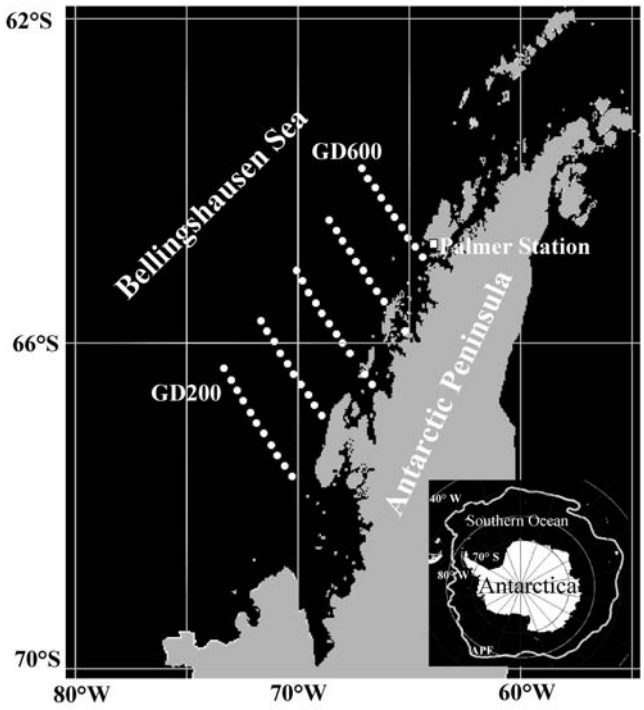

Figure 1. Geographic location of the PAL-LTER study area. Sampling locations occupied during each summer cruise are indicated with solid white circles (magenta box in lower right-hand corner inset). The five cross shelf transects are spaced every 100 km (Grid lines or GD 200 to 600). The distance between consecutive sampling locations along a grid line is 20 km, Palmer Station (64°46′ S, 64°03′ W) is symbolized with a white box, and APF is Antarctic polar front (thick solid line in figure inset).

that seasonally phytoplankton growth significantly outpaces community respiration by bacteria and zooplankton. Thus, variation in seasonal primary production is expected to be the main process responsible for annual variations of NCP in waters south of 64°S, where extensive phytoplankton blooms have been reported in the last decade [*Montes-Hugo et al.*, 2009].

[3] Climate migration along the WAP region has been described as a southward displacement of polar continental conditions (dry and cold) by subpolar maritime conditions (warm and moist) [*Smith et al.*, 2003]. These subpolar atmospheric patterns are associated with surface wind patterns marked by an increased frequency of intense (hourly average of wind speed > 20 m s^{-1}) and persistent (2–6 months) winds that have a dominant northerly component during spring-early summer in recent decades [*King and Harangozo*, 1998; *Massom et al.*, 2006, 2008]. These anomalous northerly winds are currently associated with greater snowfall, earlier sea ice retreat, compaction of sea ice floes against the coast, and freshening of the mixed layer due to sea ice and glacier melt during spring-summer [*Massom et al.*, 2006, 2008]. These changes favor early initiation of phytoplankton blooms [*Massom et al.*, 2006]. The same conditions may also drive significant declines of surface DIC and greater NCP rates in WAP surface waters.

[4] Conversely, spring-summer productivity and presumably oceanic CO_2 uptake is expected to diminish if southerlies are the dominant winds during late spring (i.e., October–November). During such years, sea ice retreat is extremely late [*Stammerjohn et al.*, 2008], and phytoplankton blooms over the shelf and offshore of the shelf break are absent [*Smith et al.*, 2008].

[5] Based on more than 10 years of in situ surveys, satellite imagery, and climate model data, we explored the following questions: (1) how many strong northerly wind events occurred in the WAP region in the last two decades, (2) to what extent do such variations in spring wind patterns affect the biological drawdown of DIC during the following summer, and (3) what is the relative contribution of sea ice and cloudiness patterns on observed DIC drawdown during midsummer? We hypothesized that midsummer depletion of salinity-corrected DIC (DIC_{Surf}*) in surface waters is enhanced during years with unusually strong and persistent spring northerly winds due mainly to an increase of primary productivity and photosynthetic DIC uptake during spring-summer months.

[6] The results of this study are organized in two sections. In section 3.1, we describe interannual variability of spring winds in terms of magnitude and direction and how those variations are associated with changes in the phytoplankton and carbonate system during summer. In addition, we characterize in detail midsummer DIC response with respect to physical and biological properties over the preceding annual cycle for two contrasting years with different spring wind patterns (strong northerly versus southerly). In section 3.2, we calculate DIC changes within the upper mixed layer of the study area during midsummer to late summer (January–February) for years dominated by relatively weak southerly or northerly winds during the preceding spring. In this analysis, we also computed contribution of primary production and sea-air CO_2 exchange to observed summer DIC variations. In section 3.3, we interpret these results in the context of decadal trends in main climate modes over the WAP region.

2. Data and Methods

2.1. In Situ Ocean Data

[7] We utilized in situ ocean data for the WAP region collected on ship-based cruises by PAL-LTER (Palmer-Long-term Ecological Research) (protocols at http://pal.lternet.edu/data/). Seawater salinity and temperature, total alkalinity, DIC, chlorophyll *a* concentration (Chl) and net primary production were obtained for January of 1994–2006 and February 1995 and 1999. Discrete field samples (all but seawater salinity and temperature) were collected over the nominal PAL-LTER sampling grid with along-shelf (~64°–68°S, 500 km) and cross-shelf (~63.4°–73.3°W, 250 km) transects (GD 200–600) spaced every 100 km and 20 km, respectively (Figure 1).

[8] CTD systems (e.g., single versus dual pump) were used to measure seawater temperature and salinity from 1993 to 2006 [*Smith et al.*, 1984; *Martinson et al.*, 1999]. Based on precruise CTD calibrations performed at SeaBird lab, the average accuracy of temperature and salinity measurements during PAL-LTER cruises was ±0.002°C and ±0.005 PSU, respectively.

[9] Samples for Chl were filtered using glass fiber filters (GF/F, Whatmann), and pigment extracts were measured by

fluorometry using the acidification method [*Smith et al.*, 1981]. Net primary production estimates were derived from daily on-deck ^{14}C-bicarbonate incubations of discrete samples [*Vernet et al.*, 2008]. Measurements were performed with water collected at different depths (100, 50, 25, 10, 5, and 1% of solar irradiance at the sea surface, wavelength = 400–700 nm) and using UV-opaque Plexiglas bottles. In the WAP region, Chl explains 60% of the variability of net primary production within the euphotic zone (P_{eu}) (Table 1) [*Dierssen et al.*, 2000, *Vernet et al.*, 2008].

[10] The upper mixed layer depth (UMLD, Table 1) was calculated using a penalty function based on a constructed S variable that exaggerates the features defining the mixed layer base [*Martinson and Iannuzzi*, 1998]. DIC was measured by coulometric determination of extracted CO_2 [*Johnson et al.*, 1987]. DIC was scaled to a constant salinity (DIC* = [35 × DIC]/salinity) for the whole PAL-LTER grid to remove the effect of freshwater from ice melt. This correction can be as high as 12% in coastal samples influenced by glacier plumes, and the bias is relatively large compared to uncorrected DIC changes during the phytoplankton growing season [*Sweeney et al.*, 2000]. Total alkalinity was determined by potentiometric titration [*Department of Energy*, 1994].

2.2. Satellite Remote-Sensing and Numerical Model Products

[11] Satellite-derived Chl (Chl_{Sat}) was obtained from remote sensing reflectance measured by SeaWiFS (Sea-viewing Wide Field-of-view Sensor) and using local bio-optical relationships calibrated with field samples ($r^2 = 0.83$, $N = 1090$) [*Dierssen and Smith*, 2000]. Daily satellite scenes over the PAL-LTER grid (4.5 × 4.5 km resolution, L2 Global Area Coverage, http://oceandata.sci.gsfc.nasa.gov) were analyzed between December and February of 1997–2006 when the zenith angle was < 65° and sea ice concentration was commonly below 10%. Monthly composites of Chl_{Sat} were calculated based on daily measurements with previous quality check (L2 flags, NASA, http://oceancolor.gsfc.nasa.gov/seadas/) [*Montes-Hugo et al.*, 2008].

[12] Sea ice concentration (SIC, 0–100%) data were derived from passive microwave satellite sensors. Two types of SIC data sets were used: (1) monthly 25 km resolution imagery from SMMR/SSM-I (The EOS Distributed Active Archive Center, DAAC, at the National Snow and Ice Data Center, NSIDC) and obtained using the Bootstrap algorithm [*Comiso*, 1995]; and (2) daily 12.5 km resolution imagery from SSM-I sensor (Ifremer-CERSAT) and processed based on daily brightness maps of NSIDC (Artist sea ice algorithm). Different sea ice products reflect distinct sea ice responses to climate variability [*Stammerjohn and Smith*, 1997]. Therefore, we chose three sea ice indexes to examine the sea ice impact on midsummer Chl and DIC: (1) NSIDC-derived sea ice extent (SIE) or the ocean area enclosed by the 15% SIC contour including a mixture of open water and pixels with 15 to 100% SIC; and (2) NSIDC-derived sea ice area (SIA) or ocean area covered only by sea ice with SIC greater than 15% [*Smith et al.*, 1998], and (3) CERSAT-derived sea ice concentration as percentage. Monthly composites of CERSAT-SIC were created from daily imagery with the Windows Imager Manager software (http://www.wimsoft.com/). Monthly wind speed (w) and direction (10 m above sea level) and cloud fraction (CF) were obtained from a climate model (Reanalysis II, Gaussian grid, 2.5° × 2.5° resolution, National Centers for Environmental Prediction-National Center for Atmospheric Research (NCEP-NCAR), NOAA). The vector winds are decomposed into zonal (u) and meridional (v) wind components, $w = \sqrt{u^2 + v^2}$.

2.3. Data Analysis and Dissolved Inorganic Carbon Budgets

[13] Monthly means were calculated for in situ (DIC* and Chl), satellite-derived (Chl_{Sat} and sea ice products), and model-based (CF and wind vectors) variables to identify the main DIC and Chl midsummer signatures and environmental drivers during years characterized by southerlies or by strong and persistent northerlies in the previous spring. Averaging of samples was done by computing the arithmetic mean of discrete samples (e.g., cruise locations, pixels) over the spatial domain of the PAL-LTER grid (10^5 km^2, Figure 1). Due to the perpendicular orientation of ship transects with respect to the coast and the coarser spatial resolution of NCEP products with respect to the in situ and satellite measurements, monthly averages of NCEP variables based on maximum and minimum geographic coordinates also included some data adjacent to the study area. This spatial bias is expected to be minor compared to aforementioned calculation errors on modeled CF and wind speed.

[14] In situ variables were used in different analyses (time series, DIC budget, seasonal DIC comparisons) based on three depth ranges: (1) 0 m to first optical depth (i.e., average penetration depth of ocean color sensors = ~20 m), and includes averaged surface Chl_{Surf}, DIC_{Surf}*, total alkalinity, water temperature and salinity for the same locations; (2) 0 m to upper mixed layer depth (UMLD ~20 to 50 m, 1993–2006 mean = 29.4 ± 2.8 m, 1 standard error) used for vertically integrated DIC* (DIC_{UML}*), and net primary production (P_{UML}); and (3) deep samples (100 m and 200–500 m depth) applied to averaged DIC* estimates for vertical diffusion and mixing terms (DIC_{100}*) and previous "winter" concentrations ($DIC_{200-500}$*) (Table 1).

[15] Influence of phytoplankton and meteorological variables on surface DIC during midsummer of years with different spring wind patterns was studied in three ways: (1) seasonal comparisons of monthly averaged data between years, (2) variation of monthly data over a full annual cycle for two case study years with extreme and opposite spring wind patterns (weak southerly with seasonal $|v|$ wind component < 3 m s^{-1}: September–November 1997 versus strong northerly with $|v|$ > 3 m s^{-1}: September–November 2001) [*Massom et al.*, 2006; *Smith et al.*, 2008], and (3) intraseasonal changes in summer DIC for 2 years dominated by relatively weak southerly or northerly winds during the preceding spring.

[16] We calculated temporal change in DIC_{UML}* and corrected for sea-air CO_2 exchange, resulting in the residual DIC* (RDIC):

$$\mathrm{RDIC} = L + VM + U + PD - \mathrm{NCP}(\mathrm{mmol\ m^{-2}d^{-1}}) \quad (1)$$

$$\mathrm{NCP} = P_{\mathrm{UML}} - M \quad (2)$$

Table 1. Definition of Oceanographic Variables and Terms Used to Calculate DIC Budget in Table 2 and Equations (1) and (2)

Symbol	Definition	Units	Relative Error (%)[a]
UMLD	Upper mixed layer depth	m	2.5[b]
Chl	Chlorophyll *a* concentration	mg m^{-3}	35[c]
Chl_{Surf}	Arithmetic average of Chl within 0–20 m depth	mg m^{-3}	
SIC	Sea ice concentration	%	10[d]
SIE	Sea ice extent	km^2	10[d]
SIA	Sea ice area	km^2	10[d]
SIA range	Difference between maximum and minimum sea ice per year	km^2	20[d]
CF	Cloud fraction	fraction of 10	15[e]
WS	Wind speed	m s^{-1}	15[e]
DIC^*_{Surf}	Arithmetic average of salinity-corrected total dissolved inorganic carbon (DIC^*) within 0–20 m depth	mmol kg^{-1}	0.3[f]
DIC^*_{100}	Arithmetic average of DIC^* measured at 100 m	mmol kg^{-1}	
$DIC^*_{200–500}$	Arithmetic average of DIC^* measured between 200 and 500 m	mmol kg^{-1}	
DIC^*_{UML}	Arithmetic average of vertically integrated DIC^* within the upper mixed layer	mmol m^{-2}	
$dDIC^*_{UML}$	Arithmetic average of DIC^*_{UML} change between January and February	mmol m^{-2} d^{-1}	0.6[f]
RDIC	Arithmetic average of $dDIC^*_{UML}$ corrected by sea-air CO_2 exchange	mmol m^{-2} d^{-1}	35
pCO_2^w	Partial pressure of CO_2 in seawater	μatm	3.3[g]
pCO_2^a	Partial pressure of CO_2	μatm	0.5[g]
F_{co_2}	Arithmetic average of net sea-to-air CO_2 flux calculated between January and February (positive, sea ⇒ air)	mmol m^{-2} d^{-1}	32[h]
P_{UML}	Arithmetic average of vertically integrated net primary production within the upper mixed layer and averaged between January and February	mmol m^{-2} d^{-1}	12[i]
P_{eu}	Net primary production within the euphotic zone	mmol m^{-2} d^{-1}	12[i]
L	Arithmetic average of lateral advection of DIC^*_{UMLD} between January and February	mmol m^{-2} d^{-1}	21[j]
VM	Arithmetic average of vertical entrainment of DIC^* into the UMLD and between January and February	mmol m^{-2} d^{-1}	25[k]
U	Arithmetic average of vertical diffusion of DIC^* into the UMLD and between January and February	mmol m^{-2} d^{-1}	25[l]
PD	Arithmetic average of net dissolution plus precipitation of $CaCO_3$ within UMLD and between January and February	mmol m^{-2} d^{-1}	>100[m]
M	Arithmetic average of DIC^*_{UMLD} production between January and February due to biological sources (remineralization of organic carbon, exudation and excretion)	mmol m^{-2} d^{-1}	>100[n]
NCP	Arithmetic average of net community production between January and February	mmol m^{-2} d^{-1}	35

[a]The relative error of the measurement is estimated for a number of replicas and based on one standard deviation normalized by the arithmetic average of the sample.

[b]Based on a water column depth of 100 m.

[c]Overall, retrieval accuracy of SIC is approximately 5 to 10% [*Comiso et al*., 1997] (see in detail SIC uncertainty terms in auxiliary material).

[d]Interference of accessory pigments (e.g., Chlorophyll *b* and *c*) can be important (up to 60% relative bias) [*Welschmeyer et al.*, 1994]. For our study area, however, the artifact on Chl measurements due to the presence of these accessory pigments is expected to be smaller (auxiliary material, Figure S1 in Text S1). SIA range is defined with respect to a Gregorian year that begins on 1 January and ends on 31 December and has a length of 365 or 366 days during an ordinary or leap year, respectively. Minimum and maximum SIA per year was generally observed during September and February, respectively.

[e]In general, there is a fair agreement between temporal variability of these NCEP products and in situ observations at Palmer Station (64°46′ S, 64°03′ W). Model-data differences for 1993–2006 show that NCEP-derived values underestimate in situ data for CF (bias up to −22.9% during December) and wind speed (up to −25.3% during February).

[f]This error corresponds to DIC precision within a depth interval of 1 m (±6 μmol Kg^{-1}, A. Dickson, UCSD, 2009). Total relative error of vertically integrated DIC within the upper mixed layer is expected to be variable depending on how deep is the UMLD. The same applies to $dDIC^*_{UMLD}$ even though twice as much uncertainty should be added since the sum of errors between initial (day in January) and final (day in February) time used to evaluate DIC changes.

[g]Relative uncertainty of partial pressure of CO_2 in seawater and air are computed with respect to a mean of 300 ppm.

[h]Fractional uncertainty of atmosphere-ocean CO_2 exchange and maximum absolute error (±1.5 mmol C m^{-2} d^{-1}) is described by [*Alvarez et al*. 2002]. Total alkalinity to calculate F_{co_2} has a precision of 0.5% (±13 μeq kg^{-1}).

[i]Relative bias of ^{14}C-based primary production estimates vary between ±4 and ±20% [*Pemberton et al*., 2006]. Vertically integrated primary production estimates are expected to have greater uncertainties depending on how many discrete samples were incubated per location and the type of interpolation technique (e.g., trapezoidal in this study) applied to calculate the integral. The euphotic zone was defined as the fraction of water column that can support photosynthesis and is illuminated in average by 1% or a greater percentage of photosynthetically available radiation (wavelength = 400–700 nm) reaching the sea surface. In the WAP region, depth of euphotic zone for 1993–2006 ranged between 20 to 100 m depth.

[j]Based on a high-resolution ocean circulation model (Parallel Ocean Program, Los Alamos National Laboratory) [*Kerbyson and Jones*, 2005], prediction error of baroclinic and barotropic currents is approximately 4%. This uncertainty on hydrodynamic calculations represents a 21% error on lateral transport of DIC assuming an averaged upper mixed layer of 50 m depth.

[k]The increase of surface DIC due to monthly changes on vertical mixing was calculated using a modified [*Peng et al.* 1987] parameterization for entrainment: $VM = (dz/\mathrm{UMLD_{Jan}}) \sum_{z=0}^{z=UMLD} (DIC^*_B - DIC^*_o)$. Here dz is ($\mathrm{UMLD_{Feb}} - \mathrm{UMLD_{Jan}}$) in m, DIC^*_B and DIC^*_o are vertically averaged concentrations of salinity-corrected DIC during January–February and calculated just below and within the summer upper mixed layer, respectively. The fractional error on vertical advection of DIC is largely related to the error in wind stress at the ocean surface, and secondary to the unknown shape of vertical velocity profiles [*Hellerman and Rosenstein*, 1983].

[l]Assuming a constant eddy diffusivity coefficient (K_z) of 5×10^{-5} m^2 s^{-1} [*Gordon et al*., 1984; *Alvarez et al*., 2002] we estimated U as: $U = -K_z\,(dDIC^*/dz)$, where ($dDIC/dz$) is the vertical DIC^* gradient between the bottom of the upper mixed layer and 100 m depth (DIC^*_{100}) and averaged for January–February. The error on vertical diffusivity of DIC was estimated as an upper bound based on water temperature diffusivity estimates [*Musgrave et al.*, 1988].

[m]Large errors for PD estimates are likely considering the relatively small contribution of pteropods and coccolithophorids to the carbonate system of WAP, and their variable sinking rates (up to 100 fold) resulting in a broad range of $CaCO_3$ dissolution rates [*Jansen et al*., 2002].

[n]Relative error on DIC remineralization estimated from particulate organic carbon decomposition rates in middepth (100–250 m) waters of Sargasso Sea [*Ono et al*., 2001] is circa 25%. However, our M estimates have an additional and unknown uncertainty (B. Schneider, personal communication, 2009) since they are derived from other terms (see equations (1) and (2)).

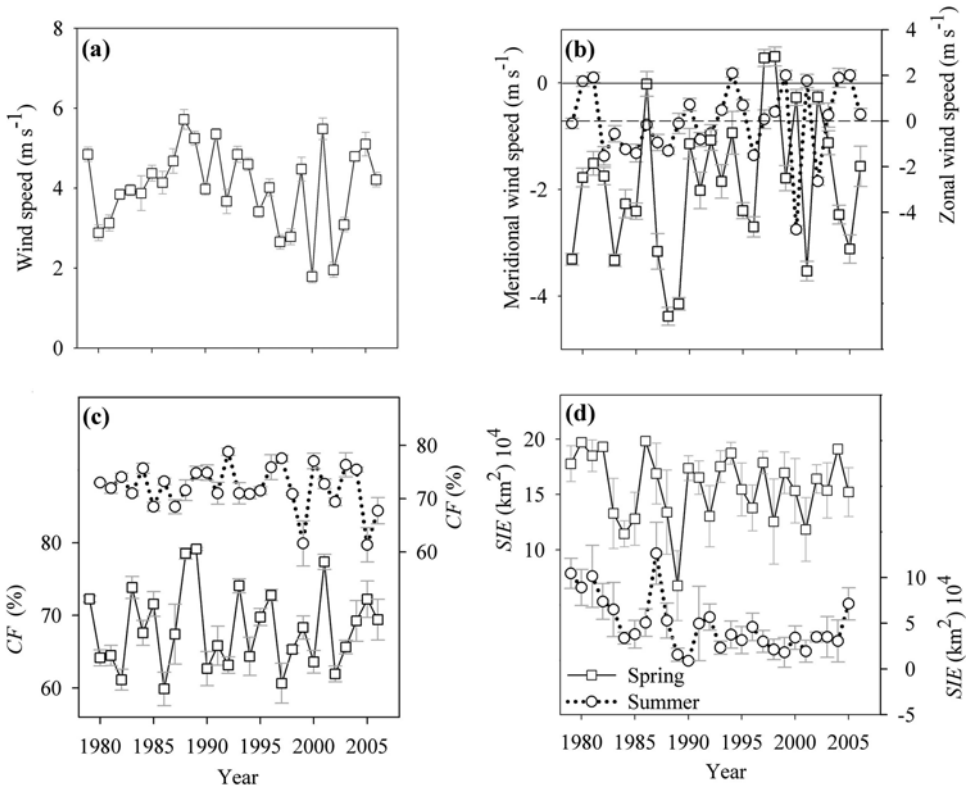

Figure 2. Interannual variability of meteorological variables averaged over the whole PAL-LTER sampling grid between 1979 and 2006. Data are shown for austral spring (September–November) and following summer (December–February) for each Austral growing season. (a) Average spring wind speed ($w = \sqrt{u^2 + v^2}$) ($N = 45$) and (b) average spring meridional winds ($N = 45$, empty rectangles and solid line, left axis) and summer zonal winds (empty circles and dotted line). Positive values above the zero horizontal lines (solid = meridional, dash = zonal) correspond to winds blowing from the south (meridional) and west (zonal), (c) average cloud fraction (CF) as percentage for spring ($N = 45$, open rectangles and solid line, left axis) and summer (open circles and dotted line, right axis), (d) average sea ice extent during spring ($N = 480$, open rectangles and solid line, right axis) and summer ($N = 480$, open circles and dotted line, left axis) of 1979–2005. Summer is plotted with respect to December's year. Error bars indicate ±1 standard error and are not visible when symbols are larger.

Each term of equations (1) and (2) is fully described in Table 1.

[17] Calculations of RDIC were made based on measurements obtained between the beginning (January) and end (February) of each cruise and over the whole PAL-LTER grid. To compare January to February, geographically coincident DIC* data were only available during January–February of 1995 and 1999. 1995 and 1999 were characterized by weak (seasonal average $|v| < 3$ m s^{-1}) northerly and southerly winds during the previous springs, respectively (Figures 2a and 2b). Although an assessment of errors for each term of equation (1) and (2) is provided in Table 1, most of these estimates are approximate and based on studies performed in other oceanic regions. DIC remineralization estimates were the most uncertain of RDIC components, thus we avoid interpreting M differences during midsummer due to spring winds or sea ice conditions. Net sea-air CO_2 flux (F_{co_2}) was calculated by multiplying the gas transfer coefficient (k_w), the CO_2 solubility in seawater (s), and the sea-air partial pressure difference of CO_2 ($dpCO_2 = pCO_2^w - pCO_2^{air}$). Values of s were derived as a function of sea surface temperature and salinity [*Weiss*, 1974], and k_w was estimated from monthly wind speed (10 m above sea level) [*Sweeney et al.*, 2007]. Partial pressure of CO_2 in seawater (pCO_2^w) was derived from DIC*, salinity-normalized alkalinity, seawater salinity and temperature (CDIAC, http://cdiac.ornl.gov/). DIC-derived pCO_2^w was not significantly different from direct pCO_2^w measurements obtained by *Takahashi et al.* [2009] (auxiliary material, Figure S2).[1] Means of atmospheric pCO_2^{air} were obtained from Jubany station (King George Island, 62° 14′S, 58° 40′W, Instituto Antártico Argentino). These monthly pCO_2^{air} values differ by −0.1% with respect to those values measured at Palmer Station between 1994 and 2002 (1978–2002 NOAA time series, http://cdiac.ornl.gov/). Differences between variable means were examined using Student's t test (H_o: $\bar{x}_1 = \bar{x}_2$) after analysis of the homogeneity of variances based on the F test. Before running Student's t test comparisons, Chl data sets were log-transformed to approximate a normal distribution. The influence of environmental variables on monthly DIC and

[1] Auxillary materials are available in the HTML. doi:10.1029/2009JC005267.

Table 2. Spearman Rank Correlations Between Chlorophyll *a* Concentration, Dissolved Inorganic Carbon, and Meteorological Variables Over the PAL-LTER Sampling Grid and During Spring and Summer[a]

Comparison	ρ	t	P
Influence of Sea Ice			
DIC^*_{Surf} (Jan)–SIA (Sep)	−0.65	−2.98	0.01*
DIC^*_{Surf} (Jan)–SIA (Dec)	−0.58	−2.48	0.03*
Impact of Meridional Winds			
Chl_{Surf} (Jan)-*v* (Oct)	−0.57	−2.40	0.03*
Chl_{Surf} (Jan)-*v*(Spring)	−0.55	4.32	<0.01**
DIC^*_{Surf} (Jan)-*v* (Oct)	0.55	2.29	0.04*
CF (Sep)-*v* (Sep)	−0.85	−5.73	<0.01**
CF (Oct)-*v* (Oct)	−0.52	−2.18	0.04*
CF (Nov)-*v* (Nov)	−0.79	−4.64	<0.01**
CF (Dec)-*v* (Dec)	−0.65	−3.11	<0.01**
Impact of Zonal Winds			
SIE (Jan)-*u* (Sep)	0.66	2.95	0.01*
SIE (Jan)-*u* (Dec)	0.60	2.52	0.03*
SIA (Jan)-*u* (Sep)	0.69	3.18	<0.01**
SIA (Jan)-*u* (Nov)	0.55	2.21	0.04*
SIA (Jan)-*u* (Dec)	0.61	2.55	0.03*
Chl_{Surf} (Jan)-*u* (Dec)	0.64	2.88	0.01*
Chl_{Surf} (Jan)-*u* (Jan)	0.60	2.60	0.02*
Chl_{Surf} (Jan)-*u* (Summer)	0.57	2.29	0.04*
CF (Nov)- *u* (Sep)	0.64	3.03	<0.01**
CF (Nov) - *u* (Oct)	0.71	3.60	<0.01**

[a]DIC^*_{Surf} and Chl_{Surf} are averaged total dissolved inorganic carbon and in situ Chl within 0–20 m depth, respectively; seasonal and monthly averages of sea ice extent (SIE), sea ice area (SIA), zonal (*u*) and meridional (*v*) wind speed components, respectively, cloud fraction (CF) are calculated during austral spring (September to November) and summer (December to February), with early summer (December) of the growing season, corresponding to previous calendar year (lag = −1 year). For each comparison, Spearman rank correlation coefficient (ρ), one-tailed *t* Student statistics with n-2 freedom degrees (*t*), and significance level *(P)* of *r* at 95% (*) or 99% (**) are also indicated.

Chl distributions between 1994 and 2006 was quantified using the Spearman rank correlation coefficient (ρ) following standardization (observation - mean)/(standard deviation) of raw values (null hypothesis is that correlation is 0). Dependency between "present" and "past" (lag = year−1) anomalies (standardized form or Z scores) was also evaluated using ρ following removal of autocorrelation effects based on phase randomization [*Ebisuzaki*, 1997].

3. Results and Discussion

3.1. Impact of Different Spring Wind Patterns on DIC, Chl, Sea Ice and Cloudiness

3.1.1. Interannual Variability

[18] Between 1979 and 2006, spring (September–November) wind intensities over the PAL-LTER sampling site were characterized by substantial interannual and decadal variations, with maximum and minimum values during 1988 and 2000, respectively (Figure 2a). Unusually strong and persistent northerly wind events (spring average $w = \sqrt{u^2 + v^2} > 3$ m s^{-1}, $|v| > 3$ m s^{-1} for ≥ 2 months) occurred during the springs of 1979, 1983, 1987–1989, 2001, and 2005 (Figure 2a and Figure 2b left axis). For spring, years with southerly winds ($v > 0$) exhibited weaker total wind speed intensity (mean $w < 3.5$ m s^{-1}) as evident during 1997 and 1998.

[19] During spring, strong northerly winds were associated with greater cloudiness (up to 15% higher CF during 1988) while weak southerly winds were coincident with lower cloud fraction values (up to −7.5% lower CF during 1997) with respect to the 1979–2006 average (66%) (Figure 2c). Cloudiness was consistently higher (>5%) during summer than spring, and year-to-year variation of summer CF was independent of wind conditions during each preceding spring (Figure 2c). For 1979–2005, SIE during spring was on average nearly 20% greater than summer values, and interannual variability of summer and spring SIE were not significantly related ($P > 0.05$) (Figure 2d). During spring, SIE was up to 57% lower when wind patterns during 1979–2005 were dominated by strong and persistent northerlies (Figures 2b and 2d). Conversely, the SIE during springs that were influenced by southerly winds was −19.9 to + 14.2% of the 1979–2005 monthly average, suggesting that the southerly wind had little influence on SIE.

[20] Between 1994 and 2006, midsummer Chl_{Surf} and DIC_{Surf}* values averaged over the whole PAL-LTER grid were sensitive to wind and sea ice patterns during summer and the previous spring (Table 2, Figures 3a and 3b). Significant drawdown of DIC_{Surf}* (up to 4% or 88 μmol Kg^{-1} with respect to preceding "winter," Z score anomaly < −1), enhancement of Chl_{Surf} (up to 4 mg m^{-3}, Z score anomaly > +0.5) and P_{eu} (up to 150 mmol m^{-2} d^{-1}, Z score anomaly > +1) during January were related to intensification of summer westerly winds (*u* up to 2 m s^{-1}, Z score anomaly anomaly > +0.5) following persistent and strong northerly wind events during spring. Those springs were also associated with increased storminess (CF up to 77.4%, CF Z score anomaly > +1.5) and earlier sea ice retreat (SIE as low as 11.8×10^4 km^2, SIE anomaly < 0) (Figures 2c, 2d, 3a, and 3b). In contrast, midsummer of years characterized by weaker southerly winds ($v > 0$) during preceding spring often presented relatively low Chl_{Surf} (as low as 0.58 mg m^{-3}, Z score anomaly < 0) and P_{eu} (as low as 20.8 mmolC m^{-2} d^{-1}, Z score anomaly < −0.5), usually high DIC_{Surf}* (up to 2229 μmol kg^{-1}, Z score anomaly > 0) in concert with weaker westerlies (*u* as low as +0.07, Z score anomaly < −0.5) during summer, and more clear days (CF low to 60.7%, Z score anomaly < −0.5) and variable SIE (12.5 to 17.8×10^4 km^2, Z score anomaly −1 to 0.7) during spring. Magnitude of surface Chl and DIC values during January of years with prior influence of weak northerly winds was variable and associated with diverse cloud and sea ice conditions.

[21] In general, midsummer DIC_{Surf}* depletions during highly productive years (e.g., January 1996 and 2002, P_{eu} = 73.3 to 100 mmolC m^{-2} d^{-1}) were not propagated to the next summer (ρ (DIC_{Surf}* versus $DIC_{Surf}{}^*_{(lag\ =\ year-1)}$) = −0.348, P = 0.472, Spearman correlation), suggesting an efficient replenishment of surface DIC during fall/winter. In Antarctic waters, surface DIC injection from deeper waters (>200 m depth) has been linked to brine rejection during sea ice formation [*Gibson and Trull*, 1999; *Sweeney* 2003] and episodic shelf intrusions of DIC-rich waters from the Antarctic Circumpolar Current (ACC) [*Martinson et al.*, 2008].

[22] Changes in midsummer Chl_{Surf} and DIC_{Surf}* fields due to strong and persistent northerly winds during the preceding spring were attributed to two main mechanisms (M1 and M2) related to changes on sea ice dynamics. In M1, anomalous low sea ice cover during spring leads to large

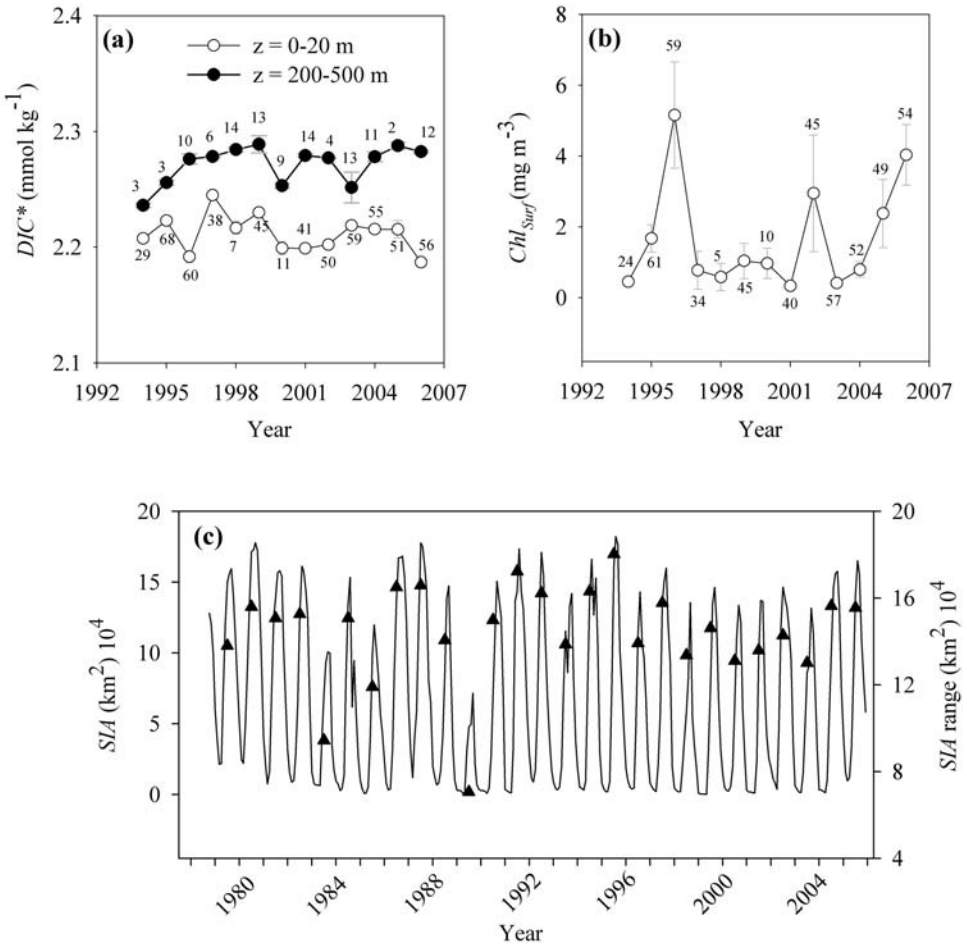

Figure 3. Interannual variability of monthly chlorophyll *a* concentration, dissolved inorganic carbon, and sea ice averaged over the whole PAL-LTER sampling grid. For January of 1994–2006, (a) monthly average of salinity-corrected total dissolved inorganic carbon measured in surface (0–20 m depth, open circles, solid line) (DIC_{Surf}*) and in deep (200–500 m depth, solid circles, solid line) ($DIC_{200–500}$*) samples, (b) Monthly chlorophyll *a* concentration measured in surface (0–20 m depth) samples (Chl_{Surf}). *N* for each year is indicated near each data point; error bars indicate (±1 standard error and are not visible when symbols are larger. (c) Monthly time-series (1979–2005) of sea ice area (SIA) (*N* = 160, solid line, left axis) and SIA range (maximum minus minimum SIA per year) (triangles, right axis).

phytoplankton blooms and autotrophic DIC removal from surface waters if water column stability during that period was mainly regulated by buoyancy forces (i.e., winter sea ice has been melted and wind-driven vertical mixing was secondary). During spring and over the PAL-LTER grid, sea ice cover has a greater influence on underwater light availability than cloudiness (Figures 2c and 2d). Therefore, a longer period with open water during this season would certainly be translated into greater light penetration to depth favoring synthesis of chlorophyll and inorganic carbon fixation by phytoplankton cells.

[23] In M2, unusual spatial distribution of sea ice during spring may result in accumulation and proliferation of phytoplankton cells nearshore of the sea ice fueling the subsequent development of extensive blooms and DIC depletion over the shelf and during summer. Atypical early retreat of sea ice during spring of 2001 had a positive feedback on midsummer phytoplankton concentrations and in situ DIC utilization by microalgae. However, phytoplankton bloom initiation and expansion did not appear to be due to greater light levels because sea ice was absent during spring. From September to October, phytoplankton was concentrated and flourished near the coast where strong and persistent northerly winds created a compact and thick marginal ice zone [*Massom et al.*, 2006]. Most of the shelf was unproductive during this period due to relatively deeper mixed layer depths originating from vigorous wind-driven vertical mixing and moderate freshening of surface waters coinciding with below average areal extent during previous winter (SIA = 8.6×10^4 km^2, annual SIA range or maximum minus minimum SIA per year = 13.6×10^4 km^2) (Figure 3c, Table 1). From November 2001 to February 2002, the localized coastal phytoplanktom bloom spread over the shelf and along the shelf break as result of increasing solar radiance and more stratified conditions caused by wind relaxation [*Massom et al.*, 2006].

[24] In general over the PAL-LTER grid, strengthening of westerly winds during summer was commonly related to

higher Chl levels during the same period (Table 2). However, intensification of westerly winds between December and February was not necessarily accompanied by strong and persistent northerly winds during the preceding spring (e.g., January of 1988 and 1989, Figure 2b). Positive effects of westerly winds on phytoplankton production and CO_2 uptake during spring-summer could be tied to circulation and sea ice distribution changes. Stronger westerly winds are expected to benefit net phytoplankton accumulation by increasing micronutrient (e.g., iron) concentrations. Surface nutrient enrichment may occur due to a greater transport of ACC filaments toward the WAP shelf and subsequent topographically induced upwelling of deep (>200 m depth) waters [*Martinson et al.*, 2008]. Indirect impact of westerly winds on midsummer Chl accumulation and photosynthetic DIC uptake may also be manifested as spatial changes on sea ice concentration (Table 2) and earlier onset of phytoplankton blooms during spring [*Massom et al.*, 2008].

[25] An alternative pattern consisting of anomalous high midsummer Chl_{Surf} and low DIC_{Surf}* preceded by weak northerly winds during spring was evident during the 1995–1996 phytoplankton growing season. January 1996 had the highest monthly averaged Chl_{Surf} (5.2 ± 1.5 mg m^{-3}, 1 standard error) and the lowest monthly DIC_{Surf}* levels (2,192 ± 5.3 μmol kg^{-1}) measured over the whole PAL-LTER grid after the 1994 growing season (Figures 3a and 3b). However, the preceding spring (September to November 1995) was dominated by relatively weak ($|v| < 3$ m s^{-1}) northwesterly winds. Between June and August of 1995, sea ice concentrations were unusually high (SIA = 14×10^4 km^2, annual SIA range = 17.1×10^4 km^2) and above the 1979–2005 winter average (SIA = 10.9 (±0.6) $\times 10^4$ km^2) (Figure 3c). Likewise, the mixed layer during midsummer of 1996 was anomalously shallow (~35.6% below the 1991–2006 average). This suggests that the large phytoplankton accumulation and DIC depletion during midsummer of 1996 may have been related to greater water column stability coincident with a thinning of the UMLD during the same period. Unlike coastal waters [*Massom et al.*, 2006], midsummer UMLD averaged over the whole PAL-LTER grid is largely controlled by freshwater inputs from sea ice melting (auxiliary material, Figure S3). Thus preceding winters with relatively large production of sea ice are likely to contribute more freshwater to the surface waters during the subsequent summer. In the WAP region, more stratified waters due to a decrease in UMLD have been associated with greater phytoplankton pigment concentrations [*Mitchell and Holm-Hansen*, 1990; *Sweeney et al.*, 2000; *Vernet et al.*, 2008], and consequently greater photosynthetic uptake of CO_2 and DIC_{Surf}* deficit due to less light limiting conditions for net phytoplankton accumulation. The positive and delayed effect of larger winter sea ice build up in the subsequent summer phytoplankton bloom has also been attributed to a larger seeding of phytoplankton during spring due to a larger release of cells originally entrapped in the sea ice matrix, to the water column after sea ice melting [*Melnikov*, 1995].

[26] The phytoplankton and CO_2 system response described during spring-summer of 1995–1996 in the PAL-LTER study area was comparable to that observed in the western Bransfield Strait (<64°S) during spring–summer of 1986–1987 [*Huntley et al.*, 1991; *Carrillo and Karl*, 1999]. Between December 1986 and February 1987, large phytoplankton concentrations (Chl > 20 mg m^{-3}) and surface DIC* as low as 1950 μmol kg^{-1} were coincident with very weak northerly winds ($|v| < 0.5$ m s^{-1}) during previous spring and easterly winds during summer. Likewise, sea ice concentrations during winter of 1986 were relatively high (SIA = 13.1×10^4 km^2, SIA range = 16.5×10^4 km^2) and above the 1979–2005 average (Figures 2d and 3c).

3.1.2. Monthly and Seasonal Variability During 2 Years With Contrasting Spring Wind Patterns

[27] Annual variation of meteorological parameters and summer monthly changes in satellite-derived Chl are depicted in Figure 4 for 2 years (1997–1998 versus 2001–2002) with atypical spring wind patterns. The choice of these two examples allowed a better differentiation of wind effects on summer DIC_{Surf} and Chl_{Surf} since maximum sea ice concentrations during winters of 1997 and 2001 were comparable and occurred during the same month (SIC Sep = 88.5%) but were associated with the different wind patterns. By spring the SIE was considerably higher in 1997 than 2001 (Figure 4a).

[28] Compared to spring of 1997, spring of 2001 was characterized by lower monthly SIC values (relative monthly change as low as −42% during October, Student's $t = 6.74$, df = 1537, $P < 0.001$, two-tail) (Figure 4a), greater wind speeds (up to threefold during October, Student's $t = 8.70$, df = 64, $P < 0.01$) (Figure 4b), and cloudier skies (CF up to 25% during November, Student's $t = 10.1$, df = 64, $P < 0.01$) (Figure 4c). However, cloudiness was higher in summer (DJF) 1997–98 than in summer 2001–02, which may have contributed to lower light levels during the peak growing season in 1997–98 than 2001–02.

[29] Compared to the southerly wind case study, the wind regime during spring of 2001 resulted in approximately a 67.5% increase in summer seasonal Chl_{Sat} (Student's $t = 3.5$, df = 4622, $P < 0.01$) and up to 86% in monthly values (February, Student's $t = 9.9$, df = 1571, $P < 0.01$) (Figure 4d). As expected, negative DIC_{Surf}* anomalies (~ –14.3 μmol kg^{-1}) were observed during January of 2002 with respect to January of 1998. Higher phytoplankton concentration in surface waters, as suggested by seasonal Chl increase, was larger during midsummer of 2002 with respect to January of 1998 due probably to lesser light limitation for net phytoplankton accumulation during midsummer of 2002. Relative decline of midsummer Chl during 1998 was also evidenced by 75% lower vertically integrated (0–100 m depth) primary production with respect to 2002. The reduced spring sea ice cover (i.e., more open water), along with less cloud cover in summer (during the peak growing season), are factors that would contribute to greater underwater light levels in 2001–02 (as compared to 1997–98) and consequently higher surface Chl and lower DIC.

[30] Based on Figure 4d, maximum phytoplankton pigment values during the midsummers of 1998 and 2002 were coincident with higher values in December than in January or February (Student's t December–January or December–February = 3.17, df = 64, $P = 0.01$). However, it is probable, based on earlier sea ice retreat during spring 2001 with respect to spring 1997, that phytoplankton Chl accumulation had an earlier beginning during the spring dominated by strong northerly winds and therefore a longer growing season. This may also explain the larger decrease of surface

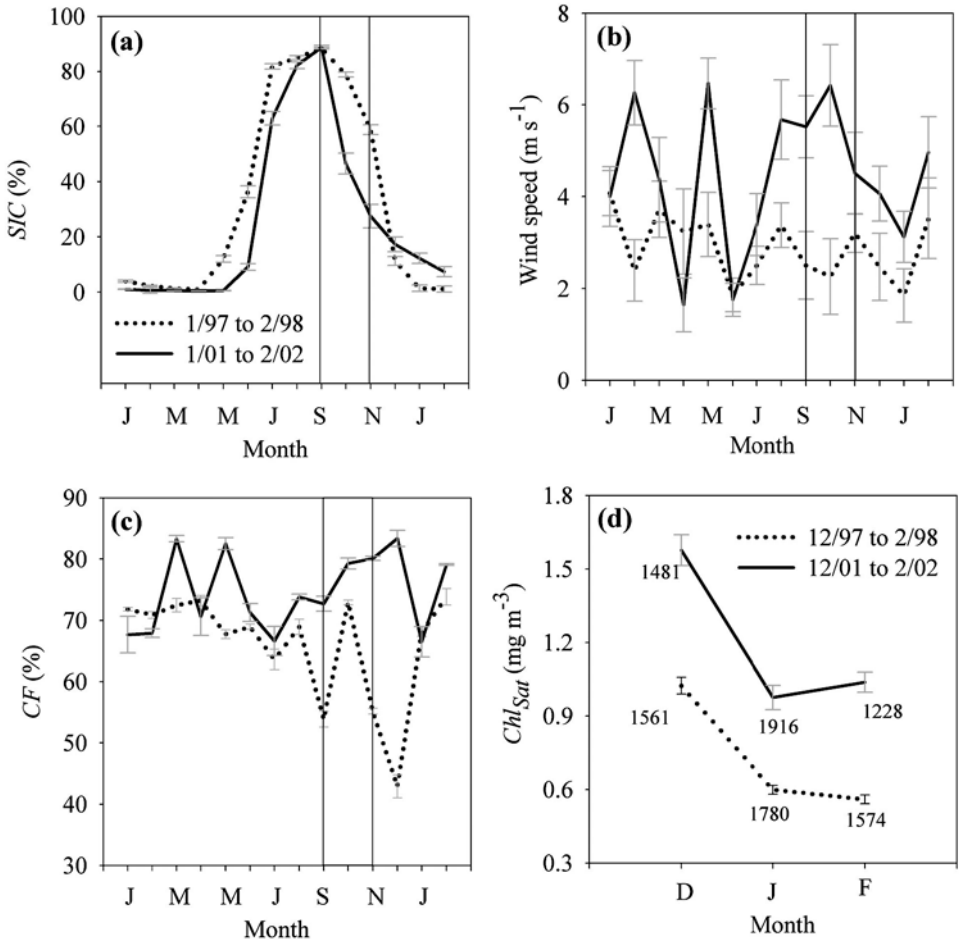

Figure 4. Monthly and seasonal variability of physical and biological properties averaged over the whole PAL-LTER sampling grid and during years with contrasting spring wind regimes. (a–c) a full annual cycle of monthly averages for January 1997 through February 1998 (dotted line) and January 2001 through February 2002 (solid line): Figure 4a sea ice concentration as percentage (SIC) (N = 640); Figure 4b wind speed ($w = \sqrt{u^2 + v^2}$, N = 15); and Figure 4c cloud fraction as percentage (N = 15). (d) The corresponding austral growing season for December 1997 through February 1998 (dotted line) and December 2001 through February 2002 (solid line) for satellite-derived chlorophyll *a* concentration (Chl_{Sat}), with number of samples placed near each data point. Ocean color data for the rest of the year are not shown since they are below the quality control imposed by SeaWiFS L2 flags (NASA, http://oceancolor.gsfc.nasa.gov/seadas/). Months between vertical solid lines correspond to the period characterized by unusually strong and persistent northerly winds during spring. For January to February, SIC comparisons between case studies are ambiguous given the calculation error using satellites (5 to 10%). Error bars indicate ±1 standard error.

DIC during summer of 2002 compared to summer of 1998 given the longer duration of phytoplankton CO_2 uptake between September 2001 and February 2002 with respect to the same period during 1997–1998.

[31] In the WAP region, *Carrillo and Karl* [1999] suggested that earlier onset of phytoplankton blooms and concomitant larger depletion of surface DIC during November–December is linked to unusually strong and persistent northerly winds during spring. They compared two periods of maximum Chl accumulation during November of 1989 (i.e., late spring with strong northerly winds and preceding winter SIA below the average) and December of 1991 (i.e., early summer with preceding weak northerlies and winter SIA above the average) (Figures 2b and 3c), and found lower DIC_{Surf} values (low as 1,950 μmol kg^{-1}) during November 1989 with respect to December 1991 (low as 2,095 μmol kg^{-1}) [*Carrillo and Karl*, 1999, Figure 6]. They also reported that phytoplankton blooms during November of 1989 began about one month earlier compared to those of 1991. This temporal shift on phytoplankton production due strong northerly winds during spring could be associated with a longer phytoplankton growing season between September 1989 and February 1990 that may be translated in lower DIC_{Surf} values during summer, and is consistent with our relatively high Chl_{Surf} and low DIC_{Surf} values measured during midsummer 2002 when preceding spring wind patterns were dominated by strong northerlies and winter SIA was below the 1979–2005 seasonal average.

Table 3. Summer Temporal Changes of Total Dissolved Inorganic Carbon in the Upper Mixed Layer of the WAP Region[a]

	January–February 1995	January–February 1999
$d\text{DIC}^*_{\text{UML}}$	−71 (101.1)	+40.6 (18.5)
RDIC	−74.6 (101.7)	+41.3 (18.6)
P_{UML}	+139.8 (13.5)	+32 (3.4)
F_{co_2}	−3.6 (0.7)	−0.7 (0.1)
$\text{WS}_{\text{Jan–Feb}}$	4.8 (0.2)	3.0 (0.3)
$\text{UMLD}_{\text{Jan–Feb}}$	28.0 (2.1)	50.0 (3.9)

[a]Mass balance calculations were based on monthly differences (February–January) and considering 10 (summer 1995) and 16 (summer 1999) locations covering the whole PAL-LTER study area. Midsummer to late summer DIC flux calculations corresponded with relatively weak (seasonal average $|v| < 3$ m s^{-1}) northerly (1995) and southerly (1999) winds during the previous spring. Between parentheses is ±1 standard error. DIC budget terms and units are described in Table 1. Arithmetic average wind speed ($\text{WS}_{\text{Jan–Feb}}$) and upper mixed layer depth ($\text{UMLD}_{\text{Jan–Feb}}$) correspond to January–February.

3.2. Effect of Spring Southerlies and Northerlies on Summer DIC Fluxes Within the Upper Mixed Layer

[32] In order to assess the effect of different spring wind patterns on temporal changes of summer DIC, we focus on the phytoplankton growing season of 1994–1995 and 1998–1999. In general, DIC_{UML}* fluxes during January–February 1995 were mainly explained by autotrophic DIC uptake by phytoplankton (Table 3). In general, more productive waters (relative change, diffr, P_{UML} = +337%, absolute change, diffa = +107.8 mmol m^{-2} d^{-1}) and DIC* depletion (diffr $d\text{DIC}_{\text{UML}}$* < −500%, diffa = −111.6 mmol m^{-2} d^{-1}) during January–February of 1995 were associated with strengthening of the westerly component of wind speed (diffr u = +428.5%, diffa = +1.7 m s^{-1}), shallower mixed layers (diffr UMLD = −44%, diffa = −22 m), and larger sea ice concentrations during previous winter (diffr SIA range = +22.1%, diffa = +3 10^4 km^2) with respect to the same period during 1999 (Figure 2 right axis, Figure 3c, Table 3).

[33] For these study cases where spring winds were relatively calm ($|u|$ and $|v| < 3$ m s^{-1}), winter sea ice concentration during 1994 (SIA = 12.8 × 10^4 km^2, well above 1979–2005 mean = 10.9 ± 0.6 10^4 km^2, 1 standard error, Figure 3c, section 3.1) was certainly the main environmental variable explaining the major role of phytoplankton photosynthesis and carbon export on controlling DIC_{UML}* during summer of 1995. In general our RDIC and P_{UML} absolute values are larger than those obtained by *Bakker et al.* [1997] (e.g., RDIC = −6.1 and P_{UML} = 20.2, mmol m^{-2} d^{-1}) and *Alvarez et al.* [2002] (RDIC = −0.3 to −29.1 and P_{UML} = 34.6 to 40.6, mmol m^{-2} d^{-1}). Due to differences in methodology and sampling design (e.g., same season but different years [*Alvarez et al.*, 2002]; transects only varying with latitude [*Bakker et al.*, 1997]), comparison of our DIC_{UML}* fluxes against other studies should be considered with caution and assuming only relative quantities.

[34] As a first approximation, the contribution of atmospheric CO_2 exchange, L, VM, U, and PD to RDIC during January–February of 1995 and 1999 can be assumed to be small compared to DIC depletion due to phytoplankton CO_2 uptake. In general, atmospheric CO_2 invasion explained a small fraction of RDIC (1.7 to 4.8%) for the two periods under study (Table 3). Based on a medium-resolution (0.4° × 0.4° bins) ocean circulation model (Parallel Ocean Program, Dr. Matthew Maltrud), we estimate that lateral advection of DIC in equation (1) could replenish on average no more than 10% of the DIC pool in the upper mixed layer of the PAL-LTER grid during January–February of 1995 and 1999 (monthly mean residual currents: $u = -0.22$ cm s^{-1}, $v = -1.04$ cm s^{-1}).

[35] Mixed layer DIC can increase due to turbulent mixing when the UMLD deepens (i.e., $\text{UMLD}_{\text{Feb}} - \text{UMLD}_{\text{Jan}} > 0$). This situation is favored in our study area by strengthening of wind speed from December to February accompanied by a weaker stratification of the upper ocean determined by relatively small contributions of freshwater derived from sea ice and glacier melting. DIC enhancement in surface waters of the PAL-LTER grid due to vertical entrainment occurred during January–February 1999 (VM = +6 mmol m^{-2} d^{-1}, dz = +20.5 m) but represented a secondary contribution to RDIC (~16%).

[36] U was twice higher during January–February 1999 (5.6 mmol C m^{-2} d^{-1}) than during January–February 1995 but, these upward fluxes of DIC never represented a significant contribution to RDIC (2 to 6%). Biological precipitation of DIC as $CaCO_3$ by pteropods and coccolithophorids is expected to be a minor and variable in the WAP region. These planktonic groups usually contribute only a small percent (<10%) to the zooplankton biomass in the Antarctic Peninsula region, and their abundance in WAP waters is reduced (10 fold, pteropods, up to 50,000 fold, coccolithophorids) compared to other Antarctic regions (e.g., Antarctic Polar Front, Weddell Sea, East Antarctica, Ross Sea) [*Iglesias-Rodriguez et al.*, 2002; *Jansen et al.*, 2002; Ross *et al.*, 2008]. Based on these relatively low densities of calcite-forming zooplankton, DIC increase due to dissolution of biogenic $CaCO_3$ is expected to be a small term of RDIC budget.

3.3. Influence of Large-Scale Atmospheric Anomalies on WAP Circulation and Surface DIC Concentrations

[37] The Southern Annular Mode (SAM), a dominant mode of atmospheric variability that describes shifts in atmospheric mass between midlatitudes and high latitudes, has been in a more positive state in the 1990s, particularly during summer–autumn, which in turn has been associated with increased northwesterly winds over the Antarctic Peninsula [*Thompson and Salomon*, 2002; *Lefebvre et al.*, 2004; *Stammerjohn et al.*, 2008]. Positive SAM index years are expected to increase DIC_{Surf}* during summer–autumn along divergent fronts (e.g., Antarctic Polar Front) and shelf-break features (e.g., deep canyons) due to changes in circulation patterns (e.g., ACC upwelling) [*Gibson and Trull*, 1999; *Lenton and Matear*, 2007; *Martinson et al.*, 2008]. In the WAP, typical positive SAM index years (e.g., 2001–2002) [*Stammerjohn et al.*, 2008] did not result in greater summer DIC_{Surf}* levels compared to negative SAM index years (e.g., 1997–1998, 2002–2003).

4. Summary and Conclusions

4.1. Impact of Spring Wind Patterns and Winter Sea Ice on Summer DIC and Chl

[38] The presence of anomalous strong and persistent northerly winds during spring is an important factor modulating the CO_2 system in surface waters of the southern

WAP region (>64°S) during spring–summer. Our results support the original working hypothesis, and a general model is suggested where higher Chl_{Surf} and lower DIC_{Surf}* concentrations during summer correspond to relatively strong and persistent northerly winds during the previous spring. This scenario is reversed during those years with relatively weak southerly or northerly winds during September–November if, during the previous winter, maximum sea ice area is within or below the long-term average.

[39] In general, most of the phytoplankton growing seasons influenced by strong and persistent northerly winds during spring had a winter SIA below the 1979–2005 average suggesting that sea ice redistribution near the coast (alternative mechanism M2) rather than increase of area with open water during spring (M1) is a more common wind-driven mechanism explaining large Chl accumulations and DIC deficit in surface waters of the PAL-LTER grid during midsummer.

[40] In the WAP, DIC_{Surf}* changes during summer are influenced by a variety of processes including photosynthesis, respiration, upwelling, and horizontal advection [*Carrillo and Karl*, 1999; *Carrillo et al.*, 2004]. Analysis of monthly changes on RDIC during midsummer to late summer of 1995 ("weak" spring northerlies) and 1999 ("weak" spring southerlies) illustrated two points: (1) the relatively larger proportion of autotrophic DIC fixation during weak northerly winds; and (2) the major importance of winter sea ice concentration in altering summer UMLD, and consequently biological (e.g., primary productivity) and physical (e.g., vertical diffusion) contributions in modulating surface DIC during years with typically weak spring winds.

4.2. Long-Term DIC Variability and Climate Modes

[41] We cannot determine the main forcing (e.g., ACC upwelling, wind during late-summer/fall, ice brine rejection and convective mixing during winter) modulating $DIC_{200–500}$* entrainment into surface waters. However, our results suggest that year-to-year variations in $DIC_{200–500}$* concentrations were relatively small and independent of the SAM polarity. Since absolute wind speed is greater during periods of anomalous northerly winds (Figures 2a and 2b) and is a major controlling factor of F_{co_2} in the Southern Ocean [*Louanchi et al.*, 2001], a greater ocean-atmosphere CO_2 exchange and concomitant effect on DIC_{Surf}* is expected during years with positive SAM index. However, and consistent with other Antarctic studies [*Carrillo and Karl*, 1999; *Carrillo et al.*, 2004; *Alvarez et al.*, 2002; *Sweeney*, 2003] changes in sea-air CO_2 exchange had only a minor influence (~10–20%) on summer DIC_{Surf}* variability.

[42] Based on DIC_{Surf}* and $DIC_{200–500}$* changes under different spring wind regimes, we conclude that the carbonate system of WAP waters (64° to 68°S) is annually resilient to biological and ice-atmosphere coupled perturbations. No "memory" effects are expected in DIC concentrations in consecutive years as DIC depletion during spring–summer is compensated by an efficient ventilation of deep water DIC during fall–winter.

[43] **Acknowledgments.** We thank Richard Iannuzzi at LDEO for processing CTD data, the Ocean Color Group at NASA for free distribution of satellite imagery, and Wesley Ebisuzaki at NOAA for his advice in interpreting NCEP-NCAR products. This research is part of the Palmer Antarctica Long-term Ecological Research Project (http://pal.lternet.edu/). It was supported by NSF OPP grants 0217282 to HWD at the Virginia Institute of Marine Science and 0823101 to HWD at the MBL.

References

Alvarez, M., A. F. Ríos, and G. Rosón (2002), Spatio-temporal variability of sea-air fluxes of carbon dioxide and oxygen in the Bransfield and Gerlache Straits during Austral summer 1995–1996, *Deep Sea Res., Part II*, *49*, 643–662, doi:10.1016/S0967-0645(01)00116-3.

Bakker, D. C. E., H. J. W. De Baar, and U. V. Bathmann (1997), Changes on carbon dioxide in surface waters during spring in the Southern Ocean, *Deep Sea Res., Part II*, *44*, 91–127, doi:10.1016/S0967-0645(96)00075-6.

Carrillo, C. J., and D. M. Karl (1999), Dissolved inorganic carbon pool dynamics in northern Gerlache Strait, Antarctica, *J. Geophys. Res.*, *104*, 15,873–15,884, doi:10.1029/1999JC900110.

Carrillo, C. J., R. C. Smith, and D. M. Karl (2004), Processes regulating oxygen and carbon dioxide in surface waters west of the Antarctic Peninsula, *Mar. Chem.*, *84*, 161–179, doi:10.1016/j.marchem.2003.07.004.

Comiso, J. C. (1995), Sea-ice geophysical parameters from SMMR and SSM/I data, in *Oceanographic Applications of Remote Sensing*, edited by M. Ikeda and F. Dobson, pp. 321–338, CRC Press, Boca Raton, Fla.

Comiso, J. C., D. Cavalieri, C. Parkinson, and P. Gloersen (1997), Passive microwave algorithms for sea ice concentration—A comparison of two techniques, *Remote Sens. Environ.*, *60*, 357–384, doi:10.1016/S0034-4257(96)00220-9.

Department of Energy (1994), Handbook of methods for the analysis of the various parameters of the carbon dioxide system in sea water, *Rep. ORNL/CDIAC-74*, ver. 2, edited by A. G. Dickson and C. Goyet, Washington, D. C.

Dierssen, H. M., and R. C. Smith (2000), Bio-optical properties and remote sensing ocean color algorithms for Antarctic Peninsula waters, *J. Geophys. Res.*, *105*, 26,301–26,312, doi:10.1029/1999JC000296.

Dierssen, H., M. Vernet, and R. C. Smith (2000), Optimizing models for remotely estimating primary production in Antarctic coastal waters, *Antarct. Sci.*, *12*, 20–32, doi:10.1017/S0954102000000043.

Ducklow, W. H., K. Baker, D. G. Martinson, L. B. Quetin, R. M. Ross, R. C. Smith, S. E. Stammerjohn, M. Vernet, and W. Fraser (2006), Marine pelagic ecosystems: The West Antarctica Peninsula, *Philos. Trans. R. Soc., Ser. B*, *362*, 67–94.

Ebisuzaki, W. (1997), A method to estimate the statistical significance of a correlation when data are serially correlated, *J. Clim.*, *10*, 2147–2153, doi:10.1175/1520-0442(1997)010<2147:AMTETS>2.0.CO;2.

Gibson, J. A. E., and T. W. Trull (1999), Annual cycle of fCO_2 under sea-ice and in open water in Prydz Bay, East Antarctica, *Mar. Chem.*, *66*, 187–200, doi:10.1016/S0304-4203(99)00040-7.

Gordon, A. L., C. T. A. Chen, and W. G. Metcalf (1984), Winter mixed layer entrainment of Weddell deep water, *J. Geophys. Res.*, *89*, 637–640, doi:10.1029/JC089iC01p00637.

Hellerman, S., and M. Rosenstein (1983), Normal monthly wind stress over the world ocean with error estimates, *J. Phys. Oceanogr.*, *13*, 1093–1104, doi:10.1175/1520-0485(1983)013<1093:NMWSOT>2.0.CO;2.

Huntley, M., D. M. Karl, P. Niiler, and O. Holm-Hansen (1991), Research on Antarctic Coastal Ecosystem Rates (RACER): An interdisciplinary field experiment, *Deep Sea Res., Part A*, *38*, 911–941, doi:10.1016/0198-0149(91)90090-3.

Iglesias-Rodriguez, D., C. W. Brown, S. C. Doney, J. Kleypas, D. Kolber, Z. Kolber, P. K. Hayes, and P. G. Falkowski (2002), Representing key phytoplankton groups in ocean carbon cycle models: Coccolithophorids, *Global Biogeochem. Cycles*, *16*(4), 1100, doi:10.1029/2001GB001454.

Jansen, H., R. E. Zeebe, and D. A. Wolf-Gladrow (2002), Modeling the dissolution of settling $CaCO_3$ in the ocean, *Global Biogeochem. Cycles*, *16*(2), 1027, doi:10.1029/2000GB001279.

Johnson, K. M., J. Sieburth, P. Williams, and L. Braendstroem (1987), Coulometric total carbon dioxide analysis for marine studies: Automation and calibration, *Mar. Chem.*, *21*, 117–133, doi:10.1016/0304-4203(87)90033-8.

Kerbyson, D. J., and P. W. Jones (2005), A performance model of the Parallel Ocean Program, *Int. J. High Performance Comput. Appl.*, *19*, 261–276, doi:10.1177/1094342005056114.

King, J. C., and S. A. Harangozo (1998), Climate change in the western Antarctica Peninsula since 1945: Observations and possible causes, *Ann. Glaciol.*, *27*, 571–575.

Lee, K. (2001), Global net community production estimated from the annual cycle of surface water total dissolved inorganic carbon, *Limnol. Oceanogr.*, *46*, 1287–1297.

Lefebvre, W., H. Goose, R. Timmermann, and T. Fichefet (2004), Influence of the Southern Annular Mode on the sea ice-ocean system, *J. Geophys. Res.*, *109*, C09005, doi:10.1029/2004JC002403.

Lenton, A., and R. J. Matear (2007), Role of the Southern Annular Mode (SAM) in Southern Ocean CO_2 uptake, *Global Biogeochem. Cycles*, *21*, GB2016, doi:10.1029/2006GB002714.

Louanchi, F., D. P. Ruiz-Pino, C. Jeandel, C. Brunet, B. Schauer, A. Masson, M. Fiala, and A. Poisson (2001), Dissolved inorganic carbon, alkalinity, nutrient and oxygen seasonal and interannual variations at the Antarctic Ocean JGFOS-KERFIX site, *Deep Sea Res., Part I*, *48*, 1581–1603, doi:10.1016/S0967-0637(00)00086-8.

Martinson, D., and R. A. Iannuzzi (1998), Antarctic ocean-ice interactions: Implications from ocean bulk property distributions in the Weddell Sea gyre, in *Antarctic Sea Ice: Physical Processes, Interactions and Variability, Antarct. Res. Ser.*, vol. 74, edited by M. O. Jeffries, pp. 243–271, AGU, Washington, D. C.

Martinson, D. G., R. A. Iannuzzi, and S. Allspaw (1999), *CTD Operations Manual-RVIB Nathaniel B. Palmer*, *Tech. Rep. LDEO97-03*, 330 pp., Antarct. Support Assoc., Englewood, Colo.

Martinson, D., S. E. Stammerjohn, R. A. Iannuzzi, R. C. Smith, and M. Vernet (2008), Western Antarctic Peninsula physical oceanography and spatio-temporal variability, *Deep Sea Res., Part II*, *55*, 1964–1987, doi:10.1016/j.dsr2.2008.04.038.

Massom, R. A., et al. (2006), Extreme anomalous atmospheric circulation in the west Antarctic peninsula region in austral spring and summer 2001/02, and its profound impact on sea ice and biota, *J. Clim.*, *19*, 3544–3571, doi:10.1175/JCLI3805.1.

Massom, R. A., S. E. Stammerjohn, W. Lefebvre, S. A. Harangozo, N. Adams, T. A. Scambos, M. J. Pook, and C. Fowler (2008), West Antarctic peninsula sea ice in 2005: Extreme ice compaction and ice edge retreat due to strong anomaly with respect to climate, *J. Geophys. Res.*, *113*, C02S20, doi:10.1029/2007JC004239.

Melnikov, I. (1995), An in situ experimental study of young sea ice formation on an Antarctic lead: Leads and polynyas, *J. Geophys. Res.*, *100*, 4673–4680.

Mitchell, M., and O. Holm-Hansen (1990), Observations and modeling of the Antarctic phytoplankton crop in relation to mixing depth, *Deep Sea Res., Part II*, *38*, 981–1007.

Montes-Hugo, M., M. Vernet, R. Smith, and K. Carder (2008), Phytoplankton size-structure on the Western shelf of the Antarctic Peninsula: A remote sensing approach, *Int. J. Remote Sens.*, *29*, 801–829, doi:10.1080/01431160701297615.

Montes-Hugo, M., S. C. Doney, H. W. Ducklow, W. Fraser, D. Martinson, S. Stammerjohn, and O. Schofield (2009), Recent changes in phytoplankton communities associated with rapid regional climate change along the West Antarctic Peninsula, *Science*, *323*, 1470–1474, doi:10.1126/science.1164533.

Musgrave, D. L., J. Chow, and W. J. Jenkins (1988), Application of a model of upper-ocean physics for studying seasonal cycles of oxygen, *J. Geophys. Res.*, *93*, 15,679–15,700, doi:10.1029/JC093iC12p15679.

Ono, S., A. Ennyu, R. G. Najjar, and N. R. Bates (2001), Shallow remineralization in the Sargasso Sea estimated from seasonal variations in oxygen, dissolved inorganic carbon and nitrate, *Deep Sea Res., Part II*, *48*, 1567–1582, doi:10.1016/S0967-0645(00)00154-5.

Pemberton, K., K. R. Clarke, and I. Joint (2006), Quantifying uncertainties associated with the measurement of primary production, *Mar. Ecol. Prog. Ser.*, *322*, 51–59, doi:10.3354/meps322051.

Peng, T. H., T. Takahashi, W. S. Broecker, and J. Olafsson (1987), Seasonal variability of carbon dioxide, nutrients and oxygen in the northern North Atlantic surface water: Observations and a model, *Tellus, Ser. B*, *39*, 439–458.

Ross, R. M., L. B. Quetin, D. G. Martinson, R. A. Iannuzzi, S. E. Stammerjohn, and R. C. Smith (2008), Palmer LTER: Patterns of distribution of five dominant zooplankton species in the epipelagic zone west of the Antarctic Peninsula, 1993–2004, *Deep Sea Res., Part II*, *55*, 2086–2105, doi:10.1016/j.dsr2.2008.04.037.

Smith, R. C., K. S. Baker, and P. Dustan (1981), Fluorometric techniques for the measurement of oceanic chlorophyll in the support of remote sensing, *Rep. SIO 81–17*, Visibility Lab., Scripps Inst. of Oceanogr., Univ. of Calif., San Diego, La Jolla, Calif.

Smith, R. C., C. R. Booth, and J. Starr (1984), Oceanographic bio-optical profiling system, *Appl. Opt.*, *23*, 2791–2797, doi:10.1364/AO.23.002791.

Smith, R. C., K. S. Baker, and S. E. Stammerjohn (1998), Exploring sea ice indexes for polar ecosystem studies, *BioSciences*, *48*, 83–93, doi:10.2307/1313133.

Smith, R. C., W. R. Fraser, and S. E. Stammerjohn (2003), Climate variability and ecological response of the marine ecosystem in the Western Antarctica Peninsula (WAP) region, in *Climate Variability and Ecosystem Response at Long-Term Ecological Research (LTER) Sites*, *D. Greenland*, edited by D. G. Goodin and R. C. Smith, pp. 158–173, Oxford Univ. Press, Oxford, U. K.

Smith, R. C., D. G. Martinson, S. E. Stammerjohn, R. Iannuzzi, and K. Ireson (2008), Bellingshausen and western Antarctic Peninsula region: Pigment biomass and sea ice spatial/temporal distributions and interannual variability, *Deep Sea Res., Part II*, *55*, 1949–1963, doi:10.1016/j.dsr2.2008.04.027.

Stammerjohn, S. E., and R. C. Smith (1997), Opposing southern ocean climate patterns as revealed by trends in sea ice coverage, *Clim. Change*, *37*, 617–639 doi:10.1023/A:1005331731034.

Stammerjohn, S. E., D. G. Martinson, R. C. Smith, and R. A. Ianuzzi (2008), Sea ice in the Western Antarctic Peninsula region: Spatio-temporal variability from ecological and climate change perspectives, *Deep Sea Res., Part II*, *55*, 2041–2058, doi:10.1016/j.dsr2.2008.04.026.

Sweeney, C. (2003), The annual cycle of surface CO_2 and O_2 in the Ross Sea: A model for gas exchange on the continental shelves of Antarctica, in *Biogeochemistry of the Ross Sea*, *Antarct. Res. Ser.*, vol. 78, edited by G. R. DiTullio and R. B. Dunbar, pp. 295–312, AGU, Washington, D. C.

Sweeney, C., D. A. Hansell, C. A. Carlson, L. A. Codispoti, L. I. Gordon, J. Marra, F. J. Millero, W. O. Smith, and T. Takahashi (2000), Biogeochemical regimes, net community production and carbon export in the Ross Sea, *Antarctica, Deep Sea Res., Part II*, *47*, 3369–3394, doi:10.1016/S0967-0645(00)00072-2.

Sweeney, C., E. Gloor, A. R. Jacobson, R. M. Key, G. McKinley, J. L. Sarmiento, and R. Wannikhof (2007), Constraining global air-sea gas exchange for CO_2 with recent bomb ^{14}C measurements, *Global Biogeochem. Cycles*, *21*, GB2015, doi:10.1029/2006GB002784.

Takahashi, T., et al. (2009), Climatological mean and decadal change in surface ocean pCO_2, and net sea-air CO_2 flux over the global oceans, *Deep Sea Res., Part II*, *56*, 554–577, doi:10.1016/j.dsr2.2008.12.009.

Thompson, D. W. J., and S. Salomon (2002), Interpretation of recent Southern Hemisphere climate change, *Science*, *296*, 895–899, doi:10.1126/science.1069270.

Vaughan, D. G., G. J. Marshall, W. M. Connolley, C. Parkinson, R. Mulvaney, D. Hodgson, J. C. King, C. J. Pudsey, and J. Turner (2003), Recent rapid climate warming on the Antarctic Peninusla, *Clim. Change*, *60*, 243–274, doi:10.1023/A:1026021217991.

Vernet, M., D. Martinson, R. Iannuzzi, S. Stammerjohn, W. Kozlowski, K. Sines, R. Smith, and I. Garibotti (2008), Primary production within the sea ice zone west of the Antarctic Peninsula: I-Sea ice, summer mixed layer and irradiance, *Deep Sea Res., Part II*, *55*, 2068–2085, doi:10.1016/j.dsr2.2008.05.021.

Weiss, R. F. (1974), Carbon dioxide in seawater: The solubility of an ideal gas, *Mar. Chem.*, *2*, 203–215, doi:10.1016/0304-4203(74)90015-2.

Welschmeyer, N. A. (1994), Fluorometric analysis of chlorophyll *a* in the presence of chlorophyll *b* and phaeopigments, *Limnol. Oceanogr.*, *39*, 1985–1992.

S. C. Doney, Department of Marine Chemistry and Geochemistry, Woods Hole Oceanographic Institution, Woods Hole, MA 02543, USA.

H. Ducklow, Ecosystems Center, Marine Biological Laboratory, Woods Hole, MA 02543, USA.

R. Frouin, Scripps Institution of Oceanography, University of California, San Diego, La Jolla, CA 92093, USA.

D. G. Martinson, Lamont-Doherty Earth Observatory, Department of Earth and Environmental Sciences, Columbia University, Palisades, NY 10964, USA.

M. Montes-Hugo and O. Schofield, Coastal Ocean Observation Lab, Institute of Marine and Coastal Sciences, School of Environmental and Biological Sciences, Rutgers-State University of New Jersey, New Brunswick, NJ 08901, USA. (montes@marine.rutgers.edu)

S. Stammerjohn, Ocean Sciences, University of California, Santa Cruz, CA 95064, USA.

C. Sweeney, Global Monitoring Division, Earth Systems Research Laboratory, National Oceanic and Atmospheric Administration, Boulder, CO 80305, USA.